Behavioral/Systems/Cognitive

Group I Metabotropic Glutamate Receptor NMDA Receptor Coupling and Signaling Cascade Mediate Spinal Dorsal Horn NMDA Receptor 2B Tyrosine Phosphorylation Associated with Inflammatory Hyperalgesia

Wei Guo,[1] Feng Wei,[1] Shiping Zou,[1] Meredith T. Robbins,[1] Shinichi Sugiyo,[1] Tetsuya Ikeda,[1] Jian-Cheng Tu,[2] Paul F. Worley,[2] Ronald Dubner,[1] and Ke Ren[1]

[1]Department of Biomedical Sciences, Dental School and Program in Neuroscience, University of Maryland, Baltimore, Maryland 21201, and [2]Department of Neuroscience, Johns Hopkins University School of Medicine, Baltimore, Maryland 21205

Hindpaw inflammation induces tyrosine phosphorylation (tyr-P) of the NMDA receptor (NMDAR) 2B (NR2B) subunit in the rat spinal dorsal horn that is closely related to the initiation and development of hyperalgesia. Here, we show that in rats with Freund's adjuvant-induced inflammation, the increased dorsal horn NR2B tyr-P is blocked by group I metabotropic glutamate receptor (mGluR) antagonists [7-(hydroxyimino)cyclopropa[b] chromen-1a-carboxylate ethyl ester (CPCCOEt) and 2-methyl-6-(phenylethynyl)-pyridine (MPEP), by the Src inhibitor CGP 77675, but not by the MAP kinase inhibitor 2′-amino-3′-methoxyflavone. Analysis of the calcium pathways shows that the *in vivo* NR2B tyr-P is blocked by an IP_3 receptor antagonist 2-aminoethoxydiphenylborate (2APB) but not by antagonists of ionotropic glutamate receptors and voltage-dependent calcium channels, suggesting that the NR2B tyr-P is dependent on intracellular calcium release. In a dorsal horn slice preparation, the group I (dihydroxyphenylglycine), but not group II [(2*R*,4*R*)-4-aminopyrrolidine-2,3-dicarboxylate] and III [L-AP 4 (L-(+)-2-amino-4-phosphonobutyric acid)], mGluR agonists, an IP_3 receptor (D-IP_3) agonist, and a PKC (PMA) activator, induces NR2B tyr-P similar to that seen *in vivo* after inflammation. Coimmunoprecipitation indicates that Shank, a postsynaptic density protein associated with mGluRs, formed a complex involving PSD-95 (postsynaptic density-95), NR2B, and Src in the spinal dorsal horn. Double immunofluorescence studies indicated that NR1 is colocalized with mGluR5 in dorsal horn neurons. mGluR5 also coimmunoprecipitates with NR2B. Finally, intrathecal pretreatment of CPCCOEt, MPEP, and 2APB attenuates inflammatory hyperalgesia. Thus, inflammation and mGluR-induced NR2B tyr-P share similar mechanisms. The group I mGluR-NMDAR coupling cascade leads to phosphorylation of the NMDAR and appears necessary for the initiation of spinal dorsal horn sensitization and behavioral hyperalgesia after inflammation.

Key words: **mGluR; MPEP; CPCCOEt; IP_3; PKC; Src; inflammation; hyperalgesia**

Introduction

Glutamate receptors (GluRs) are prominently involved in activity-dependent synaptic plasticity that may underlie the mechanisms of learning and memory and persistent pain (Malenka and Nicoll, 1999; Ren and Dubner, 1999; Woolf and Salter, 2000; Ji and Woolf, 2001). The NMDA receptor (NMDAR), a subtype of ionotropic glutamate receptors, in particular, is activated after injury and contributes to the development of spinal hyperexcitability and hyperalgesia (Haley et al., 1990; Woolf and Thompson, 1991; Dubner and Ruda, 1992). Recent studies suggest that injury-induced NMDAR activation involves tyrosine phosphorylation (tyr-P) of the NMDA receptor 2B (NR2B) subunit in the spinal dorsal horn (Guo et al., 2002a). Importantly, the increased NR2B tyr-P depends on primary afferent drive and is closely related to the development of inflammatory hyperalgesia (Guo et al., 2002a). However, the signal transduction pathways upstream to inflammation-induced NR2B tyr-P are unclear.

The interaction between the NMDAR and metabotropic GluRs (mGluRs) has received increased attention as a mechanism of modulation. Interestingly, NMDARs are physically linked to mGluRs in the postsynaptic density. The group I mGluRs bind Homer protein, and the latter binds Shank, a family of postsynaptic proteins (Tu et al., 1999). Shank also is linked to PSD-95 (postsynaptic density-95) via binding with GKAP (guanylate kinase-associated protein) (Naisbitt et al., 1999). Activation of mGluR potentiates NMDA current in dissociated rat spinal dorsal horn neurons (Cerne and Randic, 1992), *Xenopus* oocytes (Lan et al., 2001; Skeberdis et al., 2001), CA3 pyramidal cells (Benquet et al., 2002), and NMDAR-mediated synaptic transmission in rat dentate gyrus (O'Connor et al., 1994). Selective activation of mGluR1 increases NR2 subunit tyr-P in cortical neurons *in vitro* from mouse (Heidinger et al., 2002). The possible linkage of NMDAR (and NR2B

Received Nov. 24, 2003; revised Sept. 1, 2004; accepted Sept. 2, 2004.

This work was supported by National Institutes of Health Grants DE11964, DE12757, and DA10275. We thank E. B. Wade for technical assistance, Dr. Bo Xiao for his comments on this manuscript, Dr. Michael Gold for his comments on the experiments, and Novartis for providing CGP 77675 compound.

Correspondence should be addressed to Dr. K. Ren, Department of Biomedical Sciences, Room 5A26, 666 West Baltimore Street, Baltimore, MD 21201-1586. E-mail: kren@umaryland.edu.

DOI:10.1523/JNEUROSCI.3422-04.2004

 0270-6474/04/249161-13$15.00/0

phosphorylation in particular) and mGluR in the postsynaptic density in the spinal cord and their role in synaptic function are yet to be defined. In addition, the importance of mGluR-NMDAR coupling in an intact *in vivo* behavioral model of activity-dependent plasticity has not been demonstrated.

Group I mGluRs have been implicated in a variety of pain conditions associated with inflammation, neuropathy, and spinal injury (Meller et al., 1993; Mills et al., 2000; Karim et al., 2001; Walker et al., 2001; Dolan and Nolan, 2002; Hudson et al., 2002; Neugebauer, 2002; Zhang et al., 2002). The mGluR agonist-evoked response is enhanced in the spinal cord from hyperalgesic but not naive animals, and this effect is reversed by an NMDAR antagonist (Boxall et al., 1998). To test the hypothesis that mGluR-NMDAR coupling plays a role in dorsal horn hyperexcitability, we examined the upstream signaling pathways leading to NR2B tyr-P in the spinal dorsal horn in an *in vivo* model of inflammation as well as with *in vitro* methodology. The findings indicate that the ionotropic function of the NMDAR *in vivo* is subject to phosphorylation regulation that is initiated by mGluR/G-protein-linked mechanisms during injury-induced spinal dorsal horn plasticity. We further show that the inflammation- and mGluR agonist-induced NR2B tyr-P share similar mechanisms because they both require PKC, intracellular calcium release, and Src activation.

Materials and Methods

Animals. Adult male Sprague Dawley rats weighing 150–250 gm (Harlan, Indianapolis, IN) were used in all experiments. Rats were on a 12 hr light/dark cycle and received food and water *ad libitum*. To produce inflammation and hyperalgesia, complete Freund's adjuvant (CFA) (0.05–0.3 ml, 0.1 mg of *Mycobacterium tuberculosis*; Sigma, St. Louis, MO) suspended in an oil:saline (1:1) emulsion was injected subcutaneously into one or two hindpaws. The CFA injection produced an intense tissue inflammation of the hindpaw characterized by erythema, edema, and hyperalgesia (Iadarola et al., 1988; Hylden et al., 1989; Ren et al., 1992). The inflamed animals groom normally and display normal locomotor activity. They maintain their weight, explore their environment, and interact with other rats. Naive rats were used as a control. The experiments were approved by the Institutional Animal Care and Use Committee of the University of Maryland Dental School.

Spinal cord slice. Normal adult male Sprague Dawley rats weighing 150–200 gm (Harlan) were anesthetized with 2% halothane and decapitated. The lumbar spinal cord was removed quickly and kept in the cold artificial CSF (ACSF) consisting of the following (in mM): 124 NaCl, 4.4 KCl, 25 $NaHCO_3$, 2.0 $CaCl_2$, 1.0 $MgSO_4$, 1.0 NaH_2PO_4, 10 D-glucose, pH 7.4, and bubbled with 95% O_2 and 5% CO_2. Transverse spinal cord slices (600 μm thick) were cut at 4°C using a vibratome and immersed in chambers perfused at 5 ml/min with oxygenated ACSF. The slices were treated at room temperature with different drugs (see Results) to test their effect on NR2B tyr-P. At the conclusion of pharmacological treatment, the slices were homogenized to extract proteins for immunoprecipitation and Western blot analysis. In the inositol 1,4,5-triphosphate (IP_3) challenge experiment, the cellular membrane was permeabilized by a brief (10 sec) application of saponin (0.001%; Calbiochem, La Jolla, CA) to allow penetration of IP_3 through the cell membrane (Solovyova and Verkhratsky, 2003).

Western blot and immunoprecipitation. Naive and treated rats (10 min to 14 d after CFA injection) were overdosed with pentobarbital sodium (100 mg/kg, i.p.). The dorsal half of the L4–5 spinal cord tissues was removed and homogenized in solubilization buffer (50 mM Tris-HCl, pH 8.0, 150 mM NaCl, 1 mM EDTA, 1% NP-40, 0.5% deoxycholic acid, 0.1% SDS, 1 mM Na_3VO_4, 1 U/ml aprotinin, 20 μg/ml leupetin, 20 μg/ml pepstatin A). The homogenate was centrifuged at 20,200 × *g* for 10 min at 4°C, and then the supernatant was removed. The protein concentration was determined using a detergent-compatible protein assay with a bovine serum albumin standard. Each sample contained proteins from one animal. The unresolved proteins left in the pellet were verified, which included <20% of the total NR2B proteins (data not shown).

For Western blot analysis, the proteins (50 μg) were separated on a 7.5% SDS-PAGE gel and blotted to nitrocellulose membrane (Amersham Biosciences, Arlington Heights, IL) with a Trans-Blot Transfer Cell system (Bio-Rad, Hercules, CA). The blots were blocked with 5% milk in TBS buffer (20 mM Tris, 150 mM NaCl, pH 7.4) at room temperature for 30 min. After decanting the blocking buffer, the blot was incubated with the respective antibody overnight at 4°C. The membrane was washed with TBS buffer and incubated for 1 hr with anti-goat IgG horseradish peroxidase (HRP) (1:3000; Santa Cruz Biotechnology, Santa Cruz, CA) in 5% milk/TBS. The membrane was then washed three times with TBS buffer. The immunoreactivity was detected using enhanced chemiluminescence (ECL) (Amersham Biosciences). The loading and blotting of equal amount of proteins were verified by reprobing the membrane with anti-β-actin antiserum (Sigma) and with Coomassie blue staining.

For immunoprecipitation, the samples were incubated with respective antiserum overnight and then with protein A/G-Sepharose beads (Santa Cruz Biotechnology). SDS sample buffer (0.05 ml) was added to elute proteins from the protein A/G beads. The eluant was separated on SDS-polyacrylamide gel (7.5%) and transferred to a nitrocellulose membrane. To determine the level of tyr-P, the membranes were blocked and incubated with anti-phosphotyrosine 4G-10 (1:1000; Upstate Biotechnology, Charlottesville, VA) and further washed and incubated with anti-mouse IgG HRP (1:3000), and ECL was performed. The membranes were then stripped and reprobed with NR2B antiserum (1:1000). The specificity of immunoprecipitation was verified by boiling the sample before IP, thus breaking the protein–protein complex and only immunoprecipitating the target protein (Guo et al., 2002). After incubation with 4G-10, the eluted NR2B protein sample exhibited a band of 180 kDa that is the expected size for tyrosine-phosphorylated NR2B proteins. In the remaining sample that is deprived of NR2B, no specific band was identified at the 180 kDa position after incubation with 4G-10 and anti-NR2B antibodies (data not shown).

For co-immunoprecipitation of proteins associated with the NMDAR complex, the membranes were repeatedly stripped and probed with Shank (1:5000), NR2B (1:500–1000), PSD-95 (1:10,000), and Src (1:200) antibodies. GluR1 (1:500) antibody was used as a control. A set of samples was boiled for 5 min before immunoprecipitation to separate the protein complex and verify the specificity of antibodies.

The ECL-exposed films were digitized, and densitometric quantification of immunoreactive bands was performed using Scion (Frederick, MD) NIH Image 1.63. The relative tyrosine-phosphorylated protein levels were obtained by comparing the anti-phosphotyrosine immunoblot against the corresponding NR2B subunit immunoblot from the same membrane, and the deduced ratios were further normalized to that of the naive rats. This procedure avoids the variability resulting from the difference in film exposure. Data are illustrated as percentage of the naive controls. Raw data (ratio of the 4G-10 band over NR2B band) were used for statistical comparisons. ANOVA and the unpaired two-tailed *t* test were used to determine significant differences between sample groups. $p < 0.05$ was considered significant in all cases.

Immunocytochemistry. Rats were deeply anesthetized with pentobarbital and perfused transcardially with 100 ml of saline followed by 500 ml of cold (4°C) 0.1 M phosphate buffer containing 4% paraformaldehyde. The L4,5 spinal cord was removed, immersed in the same fixative overnight at 4°C, and transferred to 30% sucrose (w/v) in phosphate buffer for several days for cryoprotection. Thirty micrometer-thick sections were cut with a cryostat at −20°C. Free-floating tissue sections were incubated with rabbit anti-Shank (1:5000) or mouse anti-Src monoclonal antibodies (1:2000; Chemicon, Temecula, CA) overnight. The sections were then incubated with biotinylated goat anti-rabbit IgG or goat anti-mouse IgG (1:400; Vector Laboratories, Burlingame, CA) followed by indocarbocyanine (Cy3)-conjugated Streptavidin (1:600; Jackson ImmunoResearch, West Grove, PA). Control sections were processed with the same method except that the primary antisera was omitted or adsorbed by respective antigens.

Tyramide signal amplification (TSA) was used for double-immunofluorescent staining (Shindler and Roth, 1996; Burette et al.,

1999). After overnight incubation with the first primary antibody, rabbit anti-NR1 (1:10,000; Upstate Biotechnology), sections were reacted for 2 hr at room temperature with biotinylated secondary antibody (1:400; Jackson ImmunoResearch) followed by incubation with Streptavidin-peroxidase for 1 hr. After the application of Cy3-tyramide (PerkinElmer Life Sciences, Boston, MA), sections were washed with PBS and incubated in 4 M UREA (carbamide; in distilled water; Sigma) for 15 min. The treatment with the denaturing reagent removes the primary–secondary complex, whereas the tyramide fluorescein marker deposited on the tissue remains. The sections were then incubated with the second primary antibody, rabbit anti-mGluR5 (1:500; Upstate Biotechnology), and visualized by goat anti-rabbit IgG conjugated to Alexa Fluor 488 (1:600; Molecular Probes, Eugene, OR). After washes in PBS, sections were mounted on gelatin-coated slides and coverslipped with Vectashield (Vector Laboratories). To control for cross-reactions between the two primary antibodies, some sections were processed as above except that the second primary antibody was omitted. These sections showed normal Cy3-TSA (red) labeling but were negative on the green channel (Alexa 488). Images were collected sequentially on the Bio-Rad (LaserSharp 2000) or Zeiss (Thornwood, NY) 510 MATA laser-scanning confocal microscope.

Intrathecal procedure. The intrathecal (i.t.) cannulation was performed under methohexital anesthesia (50 mg/kg, i.p.). The atlanto-occipital membrane was exposed, and a 7–8 cm length of PE-10 tubing was inserted into the subarachnoid space through a slit made in the membrane. The cannula was advanced to the level of the lumbar spinal cord (Yaksh and Rudy, 1976). After recovery from anesthesia, animals were examined for gross signs of motor impairment. Such animals were excluded from the study. The location of the distal end of the i.t. catheter was verified visually after laminectomy at the end of the experiments. Each drug was injected in a volume of 5–10 μl followed by a flush of 10 μl of saline.

Drugs and agents. The following agents were purchased from Tocris Cookson (Ellisville, MO): group I mGluR agonist (*S*)-3,5-dihydroxyphenylglycine [(*S*)-3,5-DHPG], group II mGluR agonist (2*R*,4*R*)-4-aminopyrrolidine-2,3-dicarboxylate (APDC), group III mGluR agonist L-(+)-2-amino-4-phosphonobutyric acid (L-AP-4), mGluR1 antagonist 7-(hydroxyimino)cyclopropa[b] chromen-1a-carboxylate ethyl ester (CPCCOEt), mGluR5 antagonist 2-methyl-6-(phenylethynyl)pyridine hydrochloride (MPEP hydrochloride), ω-conotoxin GVIA [N-type voltage-dependent calcium channel (VDCC) blocker], L-type VDCC blocker nimodipine (NIMO) [(1,4-dihydro-2,6-dimethyl-4-(3-nitrophenyl)-3,5-pyridinedicarboxylic acid 2-methyloxyethyl 1-methylethyl ester], and ω-conotoxin MVIIC (non-selective VDCC blocker). The following agents were purchased from Sigma-RBI (Natick, MA): NMDA receptor channel blocker (5*R*,10*S*)-(+)-5-methyl-10,11-dihydro-5H-dibenzo[a,d]cyclohepten-5,10-imine hydrogen maleate (MK-801), NMDA receptor channel blocker ketamine hydrochloride (ketamine), and AMPA/kainate (KA) receptor antagonist 1,2,3,4-tetrahydro-6-nitro-2,3-dioxo-benzo(f)quinoxaline-7-sulfonamide disodium (NBQX). The following agents were purchased from Calbiochem: 2-Aminoethoxydiphenylborate (2APB; inhibitor of IP_3-mediated calcium release), mitogen-activated protein kinase kinase (MAPKK/MEK) inhibitor 2′-amino-3′-methoxyflavone (PD98059), PKC activator phorbol-12-myristate-13-acetate (PMA), 4α-Phorbol-12,13-didecanoate (4αPDD; inactive analog of PMA), chelerythrine chloride (PKC inhibitor), IP_3 receptor activator D-IP_3 (D-myo-inositol 1,4,5-trisphosphate, Hexasodium salt), and L-IP_3 (L-myo-inositol 1,4,5-trisphosphate, hexapotassium salt; inactive analog of D-IP_3). CGP 77675 (Src family protein tyrosine kinase inhibitor) was a gift from Novartis (Basel, Switzerland). The drugs were dissolved in saline or dimethylsulfoxide (DMSO) (Sigma), and the drug vehicle was used as a control. The doses of all agents were selected based on previous use in relevant studies.

The following antibodies were purchased: NR2B (Santa Cruz Biotechnology); 4G-10, PSD-95, Src, NR1, and mGluR5 (Upstate Biotechnology); and GluR1 (Chemicon). Shank antibodies were raised in rabbits immunized with GST fusions of Shank3 residues 1379–1740 and 1379–1675 (Tu et al., 1999).

Behavioral testing. A unilateral hindpaw inflammation was produced. Complete Freund's adjuvant (0.05 ml) suspended in an oil/saline (1:1) emulsion was injected subcutaneously into the lateral edge of one hindpaw. A set of calibrated Semmes-Weinstein monofilaments (von Frey filaments; Stoelting, Wood Dale, IL) was used to deliver mechanical stimulation. The bending force of the filaments was in a range of 9 mg to 257 gm. The testing method has been described in detail previously (Ren, 1999). Briefly, rats were habituated to stand on their hindpaws and lean against the experimenter's hand covered by a regular leather work glove. The testing filament was probed against the lateral edge of the hindpaw. The filaments were applied in an ascending series. A descending series of the filaments were used when the rat responded to the starting filament. Each filament was tested five times at an interval of a few seconds. If paw withdrawal resulting from stimulation was observed, it was registered as a response to a filament. The response frequencies [(number of responses/number of stimuli) × 100%] to a range of von Frey filament forces were determined, and a stimulus–response frequency curve was plotted. After a nonlinear regression analysis, an EF_{50} value, defined as the von Frey filament force (*g*) that produces a 50% response frequency, was derived from the stimulus–response function curve. The EF_{50} values were used as a measure of mechanical sensitivity. A cutoff value of the EF_{50} was set at 118 gm for the noninflamed paw because the responses were limited to a few high-intensity filaments with large force intervals. A reduction in EF_{50} suggests the development of mechanical allodynia, a nociceptive response to a normally non-noxious stimulus. An increase in response frequency, particularly to suprathreshold von Frey filaments, indicates mechanical hyperalgesia. ANOVA with repeated measures and *post hoc* comparisons were performed for statistical analysis. $p < 0.05$ was considered statistically significant.

Results

Inflammation induces NR2B tyrosine phosphorylation

We have shown previously that there was a rapid and prolonged increase in tyr-P, but not the protein levels, of the NR2B subunit in the spinal dorsal horn after hindpaw inflammation (Guo et al., 2002a). The increase in NR2B tyr-P was dependent on primary afferent drive because of the following: (1) the phosphorylation correlated with the temporal profile of inflammation and hyperalgesia, (2) shorter duration noxious stimulation produced a rapid and shorter-lasting increase in phosphorylation, and (3) local anesthetic block of the injected paw reversibly blocked inflammation-induced NR2B tyr-P and delayed hyperalgesia. In addition, intrathecal administration of an Src family tyrosine kinase inhibitor, 4-amino-5-(4-chlorophenyl)-7-(*t*-butyl)pyrazolo[3,4-d] pyrimidine (PP2), delayed the onset of hyperalgesia (Guo et al., 2002a). Thus, the increase in NR2B tyr-P correlated closely with the development of inflammation and hyperalgesia.

We use this *in vivo* model to examine the mechanisms of the enhanced NR2B tyr-P. The enhanced NR2B tyr-P is site specific. Comparing the effects of CFA injection on the contralateral versus ipsilateral spinal cord, we observed that at 24 hr after CFA injection, NR2B tyr-P was selectively increased in the ipsilateral spinal dorsal horn (Fig. 1). The levels of NR2B tyr-P were not affected in the contralateral lumbar spinal dorsal horn or cervical spinal cord from the same animal. Injection of saline into the hindpaw did not induce a change in tyr-P at 24 hr after injection. These findings control for the concern that NR2B phosphorylation might be attributable to nonspecific effects of stress on the animal. In the following experiments, we have expanded these findings to identify the signaling pathways involved in inflammation-induced NR2B tyr-P by using a series of receptor agonists and antagonists and kinase activator and inhibitors in both *in vivo* and *in vitro* preparations.

mGluR activation and NR2B tyrosine phosphorylation

Group I mGluRs have been implicated in a variety of pain conditions (Meller et al., 1993; Karim et al., 2001; Dolan and Nolan,

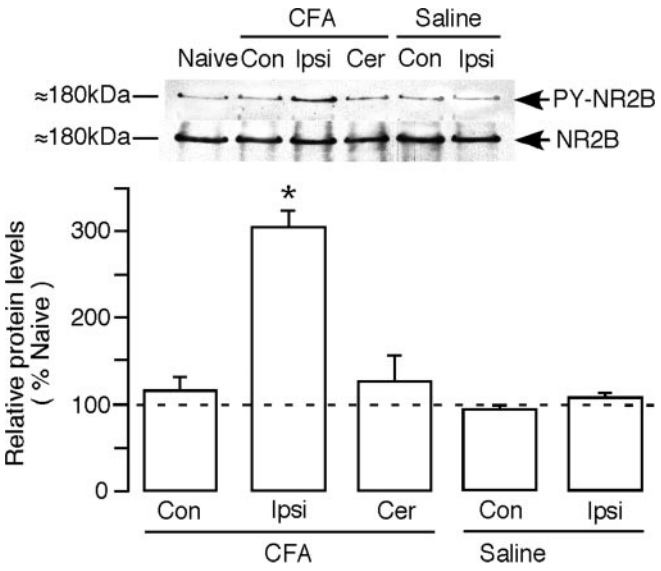

Figure 1. Selective increase in NR2B tyr-P after hindpaw inflammation. Proteins were extracted from L4,5 spinal cord of noninflamed naive (N) rats and rats at 24 hr after complete Freund's adjuvant or saline injection. The spinal dorsal horn was divided at the midline into the ipsilateral (ipsi) and contralateral (Con) halves. Cervical spinal cord (Cer) was used as a control. The top blot shows the immunoreactive bands against anti-phosphotyrosine 4G-10 (PY-NR2B) after immunoprecipitation of extracted proteins with anti-NR2B antibodies. The bottom blot shows immunobands against NR2B antibodies after stripping and reprobing the same membrane previously probed with 4G-10 antibodies. The levels of tyr-P were normalized to the respective NR2B immunoreactive bands. The relative phosphotyrosine protein levels (mean ± SEM) are expressed as a percentage of the naive controls for the purpose of illustration. Raw data were used for statistical comparisons. The asterisks indicate significant differences ($p < 0.05$) from the naive controls. $n = 5$ per time point. The dashed line indicates the control levels in noninflamed rats.

2002; Neugebauer, 2002; Zhang et al., 2002). To determine whether mGluR activation is involved in inflammation-induced NR2B tyr-P, we first examined the effect of selective group I mGluR receptor antagonists *in vivo*. An mGluR1-selective antagonist, CPCCOEt (2.0 μmol; $n = 6$), or mGluR5-selective antagonist, MPEP (170 nmol; $n = 4$), was injected intrathecally at 10 min before injection of CFA. The rats were killed at 30 min after injection of CFA, when the NR2B tyr-P reaches maximum levels (Guo et al., 2002a). Compared with the vehicle control (DMSO; 0.01 ml), the inflammation-induced NR2B tyr-P was abolished by pretreatment with CPCCOEt and MPEP (Fig. 2*A*). The basal levels of NR2B tyr-P were not affected by the same doses of CPCCOEt and MPEP (Fig. 2*C*). These results suggest a linkage between group I mGluR activation and inflammation-induced NR2B tyr-P.

Signal transduction cascade between mGluR activation and NR2B tyrosine phosphorylation

The signal pathways immediately upstream to NMDAR tyr-P involve the Src family protein tyrosine kinases (Yu et al., 1997). We have shown that inflammation-induced dorsal horn NR2B tyr-P is blocked by genistein, a nonselective tyrosine kinase inhibitor, and PP2, a selective Src family tyrosine kinase inhibitor (Guo et al., 2002a). In the present study, the involvement of Src was further examined by a potent Src inhibitor, CGP 77675. The pretreatment of CGP 77675 significantly reduced CFA-induced NR2B tyr-P *in vivo* (100 pmol; $n = 5$; $p < 0.05$) (Fig. 2*B*, left). The basal levels of NR2B tyr-P were not affected by the same dose of CGP 77675 (Fig. 2*C*). Interestingly, PD98059 (4.0 nmol; $n = 6$; i.t.), a MAPKK/MEK inhibitor, did not block inflammation-induced NR2B tyr-P (Fig. 2*B*, right), although the dose used had been shown to inhibit spinal ERK (extracellular signal-regulated kinase) activation and nociception (Ji et al., 1999). The above results suggest a sequence of events, including mGluR and Src activation and eventual NR2B tyr-P. The activity of MAP kinase, in contrast, may represent a down stream, or a parallel signaling pathway, to inflammation-induced dorsal horn NR2B tyr-P.

The Src family tyrosine kinases are activated by the proline-rich tyrosine kinase 2 (Pyk2)/cell-adhesion kinase β pathway (Dikic et al., 1996; Huang et al., 2001). PKC activation is also required for inflammation-induced NR2B tyr-P (Guo et al., 2002a). Both Pyk2 and PKC activation require an increase in intracellular calcium. One logical hypothesis is that calcium is mobilized from intracellular stores through the activation of the IP_3 pathway following mGluR activation. We directly tested this hypothesis with the administration of IP_3 receptor antagonists. As shown in Figure 3*A*, intrathecal pretreatment of 2APB (1.0 nmol; $n = 6$), a membrane permeable IP_3 receptor antagonist that does not affect Ca^{2+} release from the ryanodine-sensitive Ca^{2+} stores (Maruyama et al., 1997), blocked NR2B tyr-P after inflammation. The basal levels of NR2B tyr-P were not affected by the same doses of 2APB (Fig. 2*C*).

An increase in intracellular calcium can also be a result of an inflow of extracellular calcium through calcium-permeable channels. Because Src may mainly regulate the activity of already active NMDAR channels (Salter, 1998), we next examined the possibility that enhanced tyr-P is a feedforward regulatory mechanism triggered by inflammation-induced NMDAR activation and associated calcium influx. An NMDAR channel blocker, MK-801 (60 nmol; $n = 4$), was administered intrathecally 10 min before injection of CFA, the same procedure we used to block spinal NMDAR activation (Ren et al., 1992). The result showed that the increased NR2B tyr-P was not affected by MK-801 pretreatment (Fig. 3*B*, left). Intrathecal administration of ketamine (180 nmol; $n = 5$), an alternative NMDAR channel blocker, also did not reverse inflammation-induced increase in NR2B subunit tyr-P (data not shown). The AMPA/KA receptor channels are other potential sources of calcium for intracellular signaling, because calcium-permeable AMPA receptors exist in the superficial dorsal horn (Engelman et al., 1999). We have shown that intrathecal injection of 1.3–13 nmol of NBQX dose-dependently attenuated CFA-induced hyperalgesia (Guo et al., 2002b). However, NBQX (13 nmol; $n = 3$), an AMPA/KA receptor antagonist, did not affect CFA-induced NR2B tyr-P (Fig. 3*B*, right).

In an additional experiment, we examined the possible involvement of VDCCs in increased NR2B tyr-P. ω-conotoxin GVIA (1.3 nmol; $n = 3$; an N-type VDCC blocker), NIMO (120 nmol; $n = 3$; an L-type VDCC blocker), or ω-conotoxin MVIIC (100 nmol; $n = 4$; a nonselective VDCC blocker) were injected intrathecally 10 min before injection of CFA. DMSO (0.01 ml) was used as a vehicle control. As shown in Figure 3*C*, the mean levels of tyrosine-phosphorylated NR2B proteins were not affected by the VDCC blockers. We verified the effectiveness of the VDCC blocker treatment. Consistent with the literature (Malmberg and Yaksh, 1994; Matthews and Dickenson, 2001), intrathecal administration of nimodipine (120 nmol; $n = 4$), ω-conotoxin GVIA (1.3 nmol; $n = 4$), and ω-conotoxin MVIIC (100 nmol; $n = 4$) produced a reduction of inflammatory hyperalgesia (data not shown). Because ω-conotoxins also block a significant amount of low-voltage-activated calcium channels (LVACC currents) (McCallum et al., 2003), a role for LVACC in this effect seems unlikely. These results suggest that intracellular

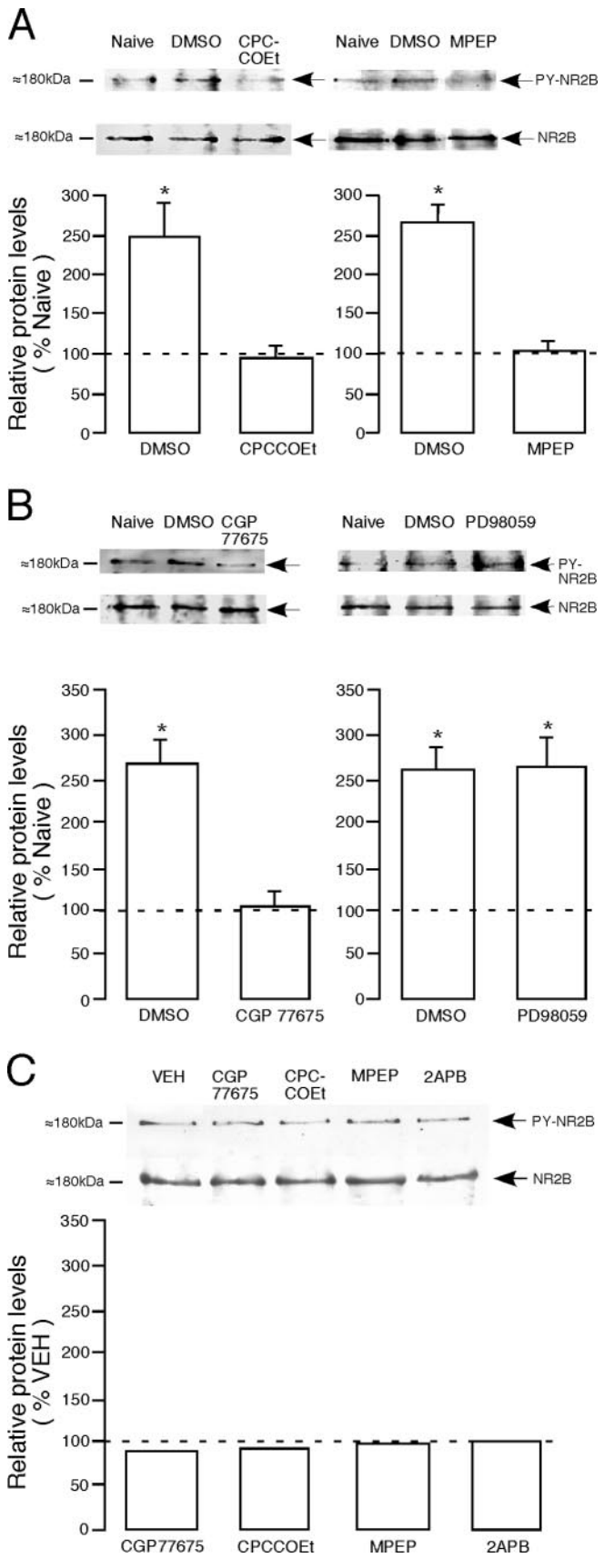

Figure 2. Inflammation-induced *in vivo* NR2B tyr-P was blocked by group I mGluR antagonists and a Src inhibitor. The drugs were injected intrathecally 10 min before CFA injection. DMSO (0.01 ml) was a vehicle control. Dorsal spinal cord tissues were collected at 30 min after inflammation of both hindpaws. In each panel, representative immunoblots against anti-4G-10 (PY-NR2B) and anti NR2B (bottom) antibodies are shown at the top. The relative levels of tyrosine-phosphorylated NR2B proteins from four individual experiments are shown below as a percentage of the naive controls (mean ± SEM). The dashed line indicates the control level. Statistical comparisons were made among all groups using raw data. *$p < 0.05$ versus naive rats. *A*, The effect of CPCCOEt (2 μmol; $n = 6$; left), an mGluR1 antagonist, and MPEP (170 nmol; $n = 4$; right), a mGluR5 antagonist. *B*, The inflammation-induced NR2B tyr-P requires Src activity. The NR2B tyr-P was blocked by intrathecal pretreatment of CGP 77675 (100 pmol; $n = 5$), an Src family protein tyrosine kinase inhibitor (left). PD98059 (4 nmol; $n = 6$; i.t.), a MAPKK inhibitor, did not prevent NR2B tyr-P after inflammation (right). *C*, The basal levels of NR2B tyr-P in naive rats were not affected by the same dose of CGP 77675, CPCCOEt, MPEP, and 2APB compared with vehicle (VEH)-treated rats ($n = 2$).

calcium mobilization but not influx through calcium-permeable channels plays a key role in inflammation-induced NR2B tyr-P.

mGluR activation *in vitro* induces NR2B tyrosine phosphorylation

The involvement of mGluR in NR2B tyr-P was next studied in an *in vitro* slice preparation by agonist challenge. Dorsal spinal cord slices were obtained from adult Sprague Dawley rats. After a 15 min incubation of the slice with DHPG (100 μM; $n = 10$), a selective group I mGluR agonist, an increase in NR2B tyr-P was observed when compared with the vehicle-treated slice ($p < 0.05$) (Fig. 4*A*). Incubation of the spinal slice with APDC (100 μM; $n = 6$), a group II mGluR agonist, or L-AP-4 (100 μM; $n = 6$), a group III mGluR agonist, did not produce a significant increase in NR2B tyr-P (Fig. 4*A*). The DHPG-induced increase in NR2B tyr-P in the spinal slice was blocked by a 10 min pretreatment with CPCCOEt (100 μM; $n = 6$) or MPEP (10 μM; $n = 6$) (Fig. 4*B*). The DHPG-induced *in vitro* NR2B tyr-P was also blocked by CGP 77675 (10 μM; $n = 6$) (Fig. 4*C*, left), a PKC inhibitor, chelerythrine (10 μM; $n = 4$) (Fig. 4*C*, middle), and 2APB (72 μM; $n = 6$) (Fig. 4*C*, right). The basal levels of NR2B tyr-P in the spinal slice were not affected by the same doses of chelerythrine, CGP 77675, CPCCOEt, MPEP, and 2APB (Fig. 4*D*). These results further suggest that group I mGluR activation is linked to NR2B tyr-P.

Agonist challenge with an IP_3 receptor agonist and PKC activation

The above findings suggest that the activation of the IP_3 pathway is necessary to induce NR2B tyr-P. This hypothesis was next tested by directly applying IP_3 receptor agonists to the spinal slice preparation. The permeabilization method was used to allow IP_3 to penetrate the cell membrane (Solovyova and Verkhratsky, 2003). The spinal slice was incubated with D-IP_3 (100 μM; $n = 4$), an IP_3 receptor activator, and L-IP_3 (100 μM; $n = 4$), an inactive analog of D-IP_3 for 15 min, and the tissues were used for immunoprecipitation and Western blot analysis. D-IP_3 induced a significant increase in NR2B tyr-P compared with the untreated (naive) slice ($p < 0.05$), whereas L-IP_3 did not produce a significant effect (Fig. 5*A*). The IP_3-induced increase in tyr-P was blocked by pretreatment with the Src inhibitor CGP 77675 (10 μM; $n = 4$) (Fig. 5*A*). We then verified whether the direct activation of PKC, a downstream event to IP_3-mediated intracellular release, could also mimic CFA-induced NR2B tyr-P. Compared with an inactive analog 4αPDD (10 μM; $n = 5$), PMA (1–10 μM; $n = 5$) produced a significant increase in NR2B tyr-P in the spinal slice ($p < 0.05$) (Fig. 5*B*). The PMA-induced NR2B tyr-P was blocked by pretreatment of the slice with CGP 77675 (10 μM; $n = 5$) and a PKC inhibitor, chelerythrine (10 μM; $n = 5$) (Fig. 5*B*).

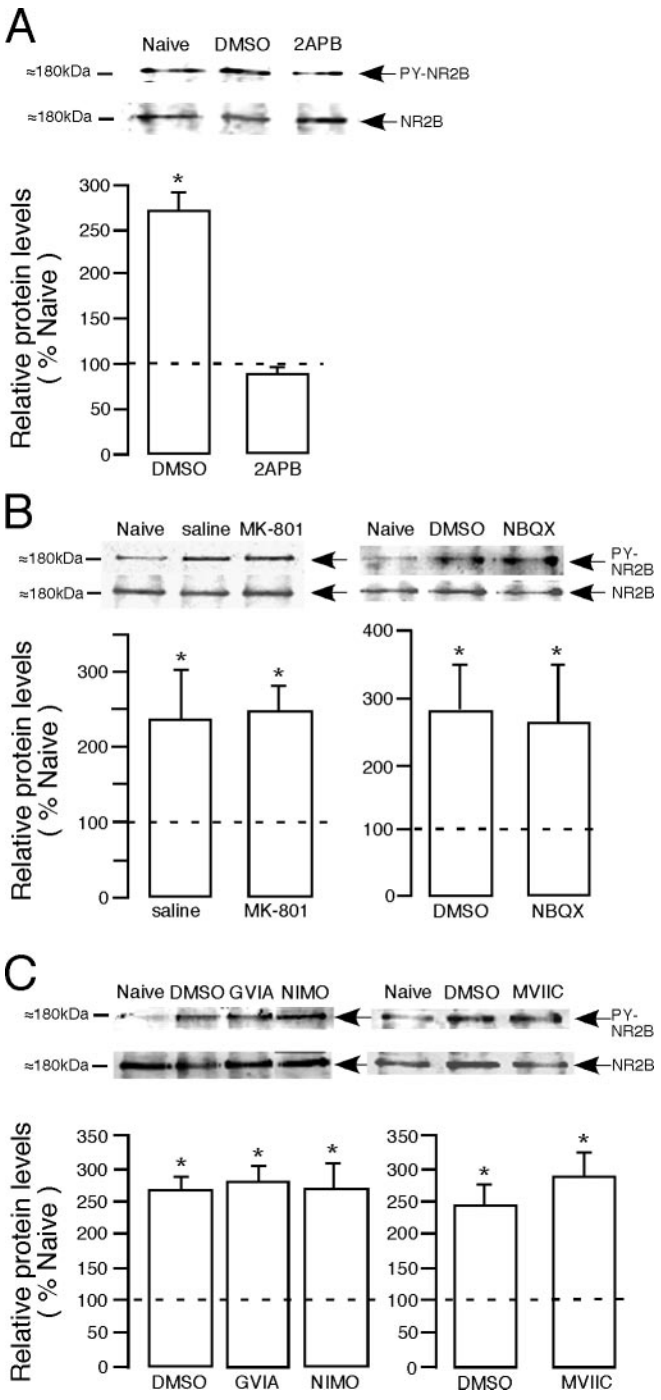

Figure 3. Contribution of calcium-releasing pathways to NR2B tyr-P. Drugs were injected intrathecally 10 min before CFA injection into the two hindpaws. DMSO (0.01 ml) and saline (0.01 ml) were vehicle controls. Dorsal horn tissues were collected at 30 min after inflammation. *A*, IP_3 receptor inhibitor 2APB (1.0 nmol; $n = 6$; right) blocked inflammation-induced NR2B tyr-P. *B*, Ionotropic glutamate receptor antagonists MK-801 (60 nmol; $n = 4$; left) and NBQX (13 nmol; $n = 3$; right) did not block NR2B tyr-P. *C*, VDCC blockers ω-conotoxin GVIA (1.3 nmol; $n = 3$; left), NIMO (120 nmol; $n = 3$; left), and ω-conotoxin MVIIC (100 nmol; $n = 4$; right) did not prevent inflammation-induced NR2B tyr-P. $^*p < 0.05$ versus naive rats.

These results further establish that activation of the IP_3-PKC pathway is sufficient to induce spinal dorsal horn NR2B tyr-P.

Src, NR2B, PSD-95, and Shank coprecipitate in the spinal dorsal horn

Previous studies suggest a link between mGluRs, NMDARs, and protein tyrosine kinase in the postsynaptic density. Coimmunoprecipitation has demonstrated the ternary or quadruple complex involving Src family protein tyrosine kinase Fyn-NR2A-PSD-95 (Tezuka et al., 1999; Lei et al., 2002), mGluR-Homer-Shank-PSD-95 (Tu et al., 1999), and Shank-GKAP-PSD-95 (Naisbitt et al., 1999) from human embryonic kidney 293 cells or rat brain. Proteomic characterization of the mouse brain has shown that the NMDAR multiprotein complex contains at least 19 proteins participating in NMDA receptor signaling (Husi et al., 2000). It is not known whether the Src-NMDAR-PSD-95 complex is directly associated with the mGluR-Homer-Shank protein complex in spinal dorsal horn postsynaptic neurons.

To assess the molecular basis of mGluR-NMDAR interaction underlying inflammation-induced NR2B tyr-P, we determined whether the NR2B subunit of the NMDAR is linked to tyrosine kinase and proteins associated with mGluRs in the spinal dorsal horn. Total proteins were extracted from spinal dorsal horn tissues and were coimmunoprecipitated with antibodies recognizing Src, Shank, NR2B, or PSD-95. All four proteins were present in the spinal dorsal horn (Fig. 6, left blots). Shank was represented as a 210 kDa band (Tu et al., 1999) followed by NR2B at 180 kDa, PSD-95 at 95 kDa, and Src at 60 kDa.

When antibodies recognizing Src were used to immunoprecipitate, Shank, NR2B, and PSD-95 were also detected in immunoprecipitates after repeated stripping and probing (Fig. 6, middle blots). Similarly, Shank antibodies coprecipitated NR2B, Src, and PSD-95 (Fig. 6, right blots). In contrast, GluR1 proteins were not coprecipitated (Fig. 6). Boiling tissue extracts before immunoprecipitation interrupted the coimmunoprecipitation of associated proteins, leaving only Src or Shank in the immunoprecipitates (Fig. 6, left two lanes of the middle and right blots). Similar results were obtained when NR2B-selective or PSD-95-selective antibodies were used for immunoprecipitation (data not shown). These results indicate that Shank, a protein closely associated with mGluRs, is also associated with a complex that includes Src protein tyrosine kinase, NR2B, and PSD-95.

The complex involving Src, NR2B, PSD-95, and Shank is likely a postsynaptic structure in intrinsic spinal neurons, because spinal PSD-95 is not present in dorsal root ganglion neurons and is not affected by spinal nerve axotomy and dorsolateral funiculus lesions (Tao et al., 2000). NR2B and PSD-95 immunoreactivity has been observed in the superficial laminas of the dorsal horn (Boyce et al., 1999; Tao et al., 2000). The Shank- and Src-like immunoreactivity is also intensely localized to rat spinal dorsal horn neurons (Fig. 7). Densely stained cell bodies are observed in the superficial (Fig. 7*C*,*C1*,*D*,*D1*) and deep (Fig. 7*C*,*C2*,*D*,*D2*) dorsal horn, a key structure in initial nociceptive processing. Numerous ventral horn neurons also exhibited Shank and Src immunoreactivity (Fig. 7*A*,*B*).

Double immunofluorescence studies indicated that NMDAR colocalized with mGluR in dorsal horn neurons (Fig. 8). Figure 8*A–C* shows that in the lateral lamina V of the dorsal horn, many NR1-labeled neurons (red) overlap with mGluR5-positive neurons (green). The NR1 staining often exhibited punctate profiles in the cell membrane, dendrite, and cytoplasm (Fig. 8A_1). The mGluR5-like immunoreactivity, in contrast, appeared uniformly in the cell membrane and cytoplasm (Fig. 8B_1). Immunoprecipitation analysis further indicated that mGluR5 proteins coimmunoprecipitated with NR2B proteins (Fig. 8*D*). These results provide anatomical and biochemical evidence that supports the signal coupling of mGluR with NMDAR in the spinal dorsal horn.

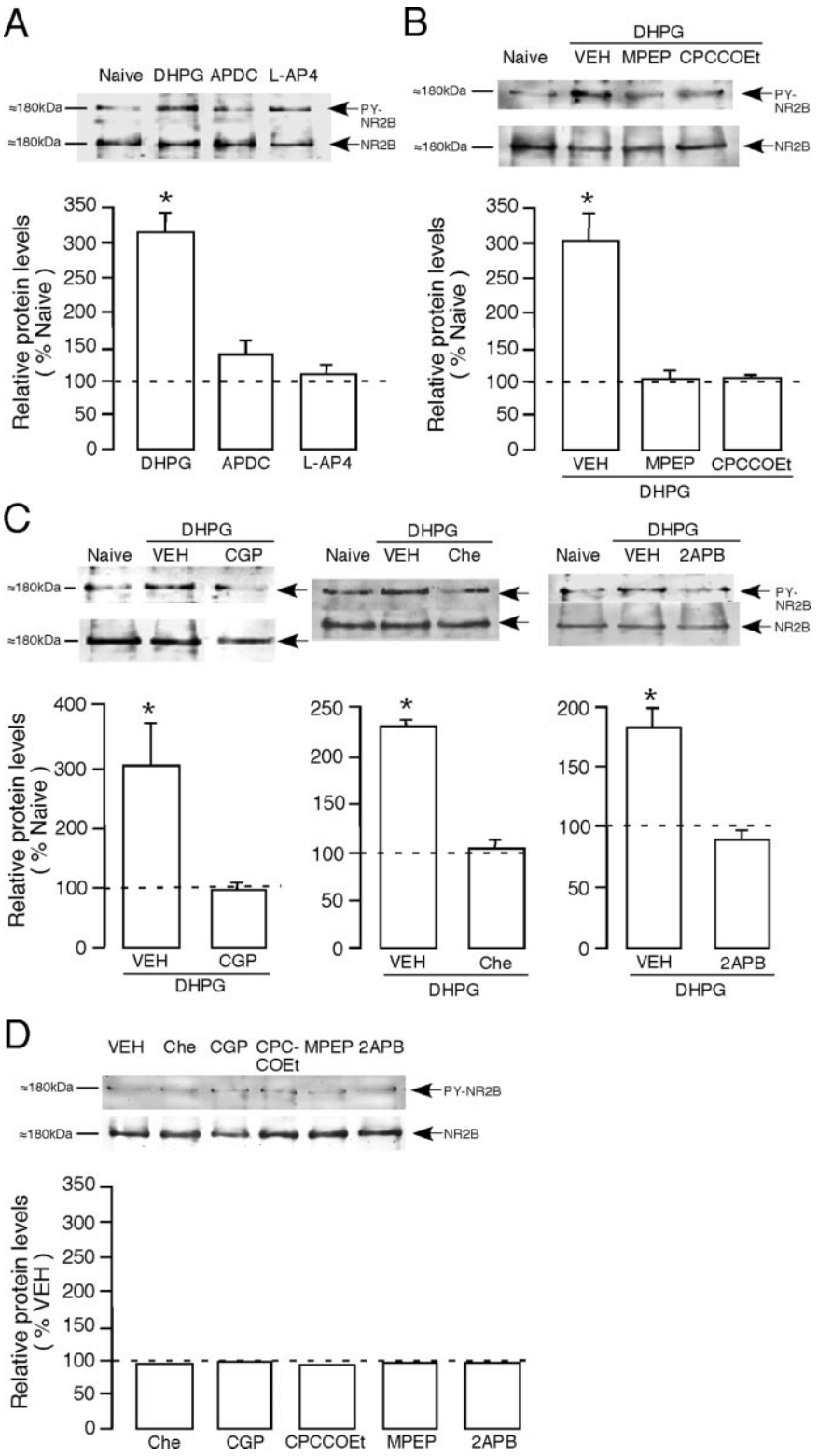

Figure 4. The mGluR agonists induced NR2B tyr-P *in vitro*. The transverse spinal cord slice was obtained from adult 8- to 10-week-old rats. Spinal slices were incubated with drugs for 15 min before protein extraction. In all panels, representative immunoblots against anti-4G-10 (PY-NR2B) and anti-NR2B antibodies are shown at the top, and mean relative levels of tyrosine-phosphorylated NR2B proteins are shown in the bar graphs. The dashed line in the bar graphs indicates the percentage of naive level. *$p < 0.05$ versus naive untreated slices. *A*, Selective group I (DHPG; 100 μM; $n = 10$) but not group II (APDC; 100 μM; $n = 6$) and group III (L-AP-4; 100 μM; $n = 6$) mGluR agonists induced NR2B tyr-P in spinal slice. DHPG-induced NR2B tyr-P was blocked by CPCCOEt (100 μM; $n = 6$) and MPEP (10 μM; $n = 6$) (*B*), an Src inhibitor, CGP 77675 (CGP; 10 μM; $n = 6$) (*C*, left), a PKC inhibitor, chelerythrine (Che; 10 μM; $n = 4$) (*C*, middle), and an IP_3 receptor inhibitor 2APB (72 μM; $n = 6$) (*C*, right). *D*, The basal levels of NR2B tyr-P in naive rats were not affected by the same dose of Che, CGP 77675, CPCCOEt, MPEP, and 2APB compared with vehicle (VEH)-treated rats ($n = 2$).

Group I mGluR antagonists and IP_3 receptor inhibitor attenuate inflammatory hyperalgesia and allodynia

We next examined whether the antagonism of group I mGluRs and IP_3 receptors affected the initiation and maintenance of inflammatory hyperalgesia. Behavioral hyperalgesia, an exaggerated nocifensive response to a noxious stimulus, and allodynia, pain induced by a normally non-noxious stimulus, develop quickly after hindpaw inflammation (Guo et al., 2002a). We assessed mechanical hyperalgesia and allodynia of the hindpaw according to the study by Ren (1999). A series of calibrated von Frey filaments with bending forces ranging from 0.009 to 257 gm were applied to the hindpaw skin surface. An active withdrawal of the paw from the probing filament was defined as a response. Each von Frey filament was applied five times at intervals of a few seconds. The response frequencies to the range of von Frey filament forces were determined, and stimulus–response frequency curves were plotted (Fig. 9*A*). This stimulus–response frequency curve represents responses to threshold as well as suprathreshold stimuli and an EF_{50} value, defined as the von Frey filament force (g) that produces a 50% response frequency, can be derived after a nonlinear regression analysis. Before injection of CFA, there was no significant difference between the baseline stimulus–response frequency curves for different groups of animals, indicating consistent responses to von Frey filaments (Fig. 9*A*, pre-CFA). After the CFA injection, there was a leftward shift of the curve (Fig. 9*A*) (30 min vehicle vs baseline vehicle). The shift of the stimulus–response frequency function curve after inflammation indicates an increased response to suprathreshold stimuli and a decrease in EF_{50} value. These inflammation-induced changes suggest the presence of mechanical hyperalgesia and allodynia, because there was an increase in response to suprathreshold stimuli and a decreased response threshold for nocifensive behavior. Also shown in Figure 9*A*, pretreatment of two group I mGluR antagonists, CPCCOEt (2 μmol) and MPEP (170 nmol), resulted in a rightward shift of the stimulus–response curves (Fig. 9*A*, 30 min post-CFA), suggesting an almost complete reversal of behavioral hyperalgesia and allodynia. At 2 hr post-CFA, the hyperalgesia and allodynia were partially recovered as indicated by a leftward shift of the stimulus–response curves (Fig. 9*A*) (2 hr CPCCOEt/MPEP vs 30 min CPCCOEt/MPEP).

The effects of mGluR antagonists and an IP_3 receptor inhibitor on mechanical

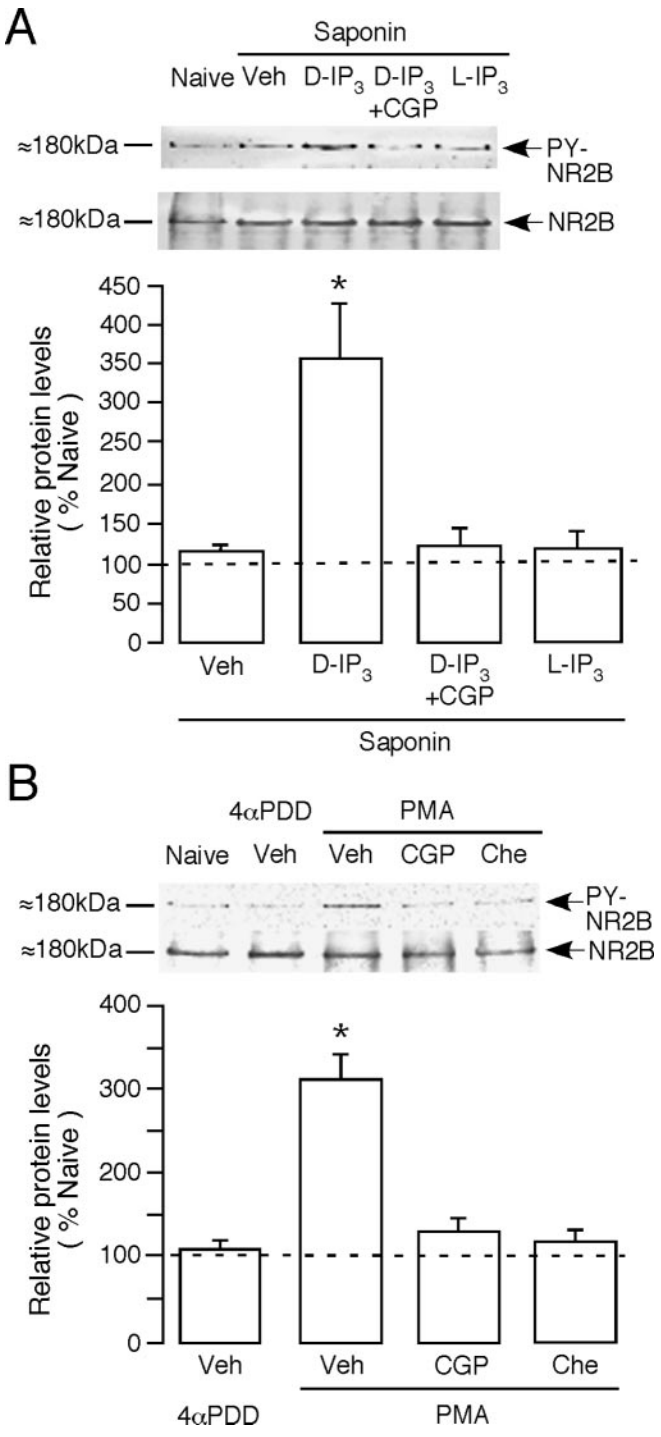

Figure 5. IP_3 and PMA induced NR2B tyr-P *in vitro*. *A*, D-IP_3 (100 μM; $n = 4$), an IP_3 receptor activator, induced a significant increase in NR2B tyr-P compared with untreated (naive) slices. The increased NR2B tyr-P was blocked by pretreatment with CGP 77675 (10 μM; $n = 4$). L-IP_3 (100 μM; $n = 4$), an inactive analog of D-IP_3, did not produce a significant effect. The slices were permeabilized by exposure to a brief (10 sec) application of saponin (0.001%) to allow penetration of IP_3 through cell membrane. Saponin itself [saponin plus vehicle (Veh)] did not affect the level of NR2B tyr-P. *B*, Direct application of PMA to spinal slices to activate PKC, a downstream event to IP_3-mediated intracellular release, also mimicked CFA-induced NR2B tyr-P. PMA (1 μM; $n = 5$) produced a significant increase in NR2B tyr-P in the spinal slice. The inactive analog 4αPDD (10 μM; $n = 5$) did not produce a significant effect. The PMA-induced NR2B tyr-P was blocked by inhibitors of Src (CGP 77675, 10 μM) and PKC [chelerythrine (Che)]. *$p <$ 0.05 versus naive untreated slices.

hyperalgesia and allodynia were quantified by comparing the EF_{50} values (Fig. 9*B*,*C*). In pretreatment experiments, the EF_{50} values of the inflamed paw were significantly increased in CPCCOEt-treated (2 μmol; $n = 5$), MPEP-treated (170 nmol; $n = 5$), or 2APB-treated (1 nmol; $n = 6$) rats to pre-CFA levels at 1–30 min after inflammation when compared with vehicle-treated rats and to pre-CFA controls (Fig. 9*B*). At 2 hr time points, the EF_{50} values did not show a significant difference from the vehicle-injected rats, although they appeared to remain at an elevated level. In post-treatment experiments, mechanical hyperalgesia–allodynia was determined at 1 d after CFA injection and then CPCCOEt (2 μmol; $n = 4$), MPEP (170 nmol; $n = 5$), or 2APB (1 nmol; $n = 6$) were intrathecally injected. The post-treatment with CPCCOEt and MPEP produced a slight increase in EF_{50} values of the inflamed paw that lasted for ~5 min (Fig. 9*C*). The post-treatment with 2APB did not produce an effect on hyperalgesia. Thus, compared with pretreatment, the post-treatment of mGluR antagonists appeared to be less effective in reversing inflammatory hyperalgesia. There was no effect of the mGluR antagonists on mechanical responses of the contralateral noninflamed paw in either pretreatment or post-treatment paradigm (Fig. 9*B*,*C*). These results suggest that the activation of the group I mGluRs is important for the initiation but plays less of a role in the maintenance of inflammatory hyperalgesia.

Discussion

The present study addresses signal pathways that mediate *in vivo* NR2B tyr-P in the spinal dorsal horn in a model of inflammation and hyperalgesia. We extend previous findings by showing that administration of selective group I mGluR antagonists completely blocks NR2B tyr-P as well as mechanical hyperalgesia and allodynia after inflammation. In addition, in an *in vitro* spinal dorsal horn slice preparation, application of group I mGluR agonists produces NR2B tyr-P that mimics the CFA-induced *in vivo* effect. Importantly, additional analysis in both the *in vivo* inflammatory hyperalgesia model and the *in vitro* model indicate that IP_3 receptor-mediated intracellular calcium release and Src family kinases play a critical role in triggering the cascade that leads to NR2B tyr-P. These findings suggest that the activation of mGluRs is key to initiating an enhanced NMDAR response after tissue injury. Thus, the ionotropic function of the NMDAR *in vivo* is subject to tyr-P regulation that is initiated by mGluR/G-protein-linked mechanisms during inflammation-induced spinal dorsal horn plasticity. The hypothesis that the induction of spinal dorsal horn sensitization after inflammation is related primarily to activity of NMDA, AMPA, NK-1, and Trk B receptors (Woolf and Salter, 2000; Hunt and Mantyh, 2001) needs to be revised in light of the present findings.

The spinal dorsal horn is the major site for initial nociceptive processing. Our coimmunoprecipitation experiments suggest that in the dorsal horn, mGluR-Homer-Shank complex and NMDARs are biochemically linked through related postsynaptic density proteins such as PSD-95 and Shank. In addition, this super protein complex also includes Src family protein tyrosine kinases (Tezuka et al., 1999; Lei et al., 2002; our results) that are important modulators of NMDAR channels (Yu et al., 1997). Accordingly, the NR2B subunit may be phosphorylated by kinases intrinsic to this protein complex. The mGluR-NMDAR coupling in dorsal horn neurons is supported by the fact that selective mGluR antagonists block inflammation-induced NR2B tyr-P and selective mGluR agonist-induced NR2B tyr-P in spinal slices. Previous studies have shown that activation of group I mGluRs enhances NMDA-induced currents (Cerne and Randic,

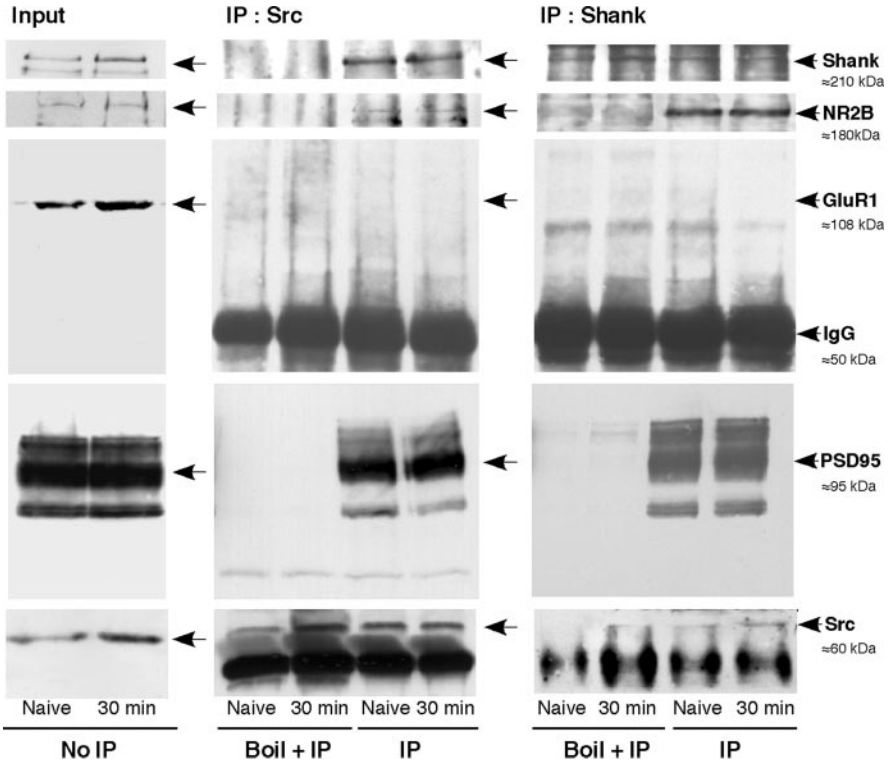

Figure 6. Coimmunoprecipitation (IP) of Shank, NR2B, PSD-95, and Src in the spinal dorsal horn. Spinal dorsal horn tissues were taken from naive rats and inflamed rats at 30 min after injection of CFA into the hindpaw. Proteins were immunoprecipitated with Src (middle) or Shank (right) antibodies and probed with antibodies against Shank, NR2B, GluR1, PSD-95, and Src. Note that boiling of the samples before IP eliminated associated proteins, leaving only Src (middle, bottom) of Shank (left, top) that was directly pulled down by respective antibodies. GluR1 protein was not coimmunoprecipitated with Src or Shank antibodies.

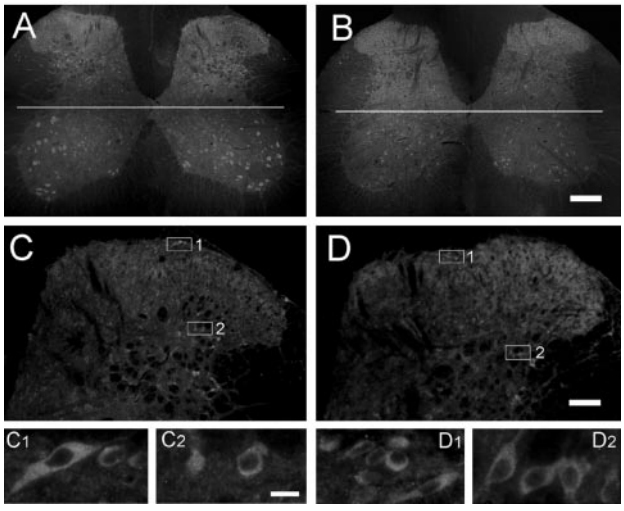

Figure 7. Immunohistochemical localization of Shank and Src in the spinal cord of the rat. Shank-like (*A*, *C*) and Src-like (*B*, *D*) immunoreactivity is distributed in spinal neurons. Low-power views of the lumbar spinal cord are shown in *A* and *B*. The horizontal lines in *A* and *B* separate the spinal cord into the dorsal (top) and ventral (bottom) halves. The dorsal half of the spinal cord was used for phosphorylation analysis. *C* and *D* show enlarged fields of dorsal horn from *A* and *B*, respectively. C_{1-2} and D_{1-2} illustrate images enlarged from the respective superficial (C_1, D_1) and deep (C_2, D_2) dorsal horn regions in *C* and *D*, indicated by small rectangles. Scale bars: *A*, *B*, 0.4 mm; *C*, *D*, 0.2 mm; C_{1-2}, D_{1-2}, 0.025 mm.

1992; Bond and Lodge, 1995) and the NMDA-mediated increase in intracellular calcium concentration in dorsal horn neurons (Bleakman et al., 1992). A role of mGluR in central sensitization and persistent pain has been suggested previously (Morisset and Nagy, 1996; Neugebauer et al., 1999; Karim et al., 2001). The present study further shows that the effects of mGluR agonists are coupled to NR2B phosphorylation and that the inflammation- and mGluR agonist-induced NR2B tyr-P share similar mechanisms, because they both require PKC (Guo et al., 2002a), intracellular calcium release, and Src activation.

It is known that activation of group I mGluRs produces nocifensive behaviors in rats (Lorrain et al., 2002), although the mechanisms of these effects were unclear. A number of studies have indicated a role of group I mGluRs in central sensitization and hyperalgesia (Fisher and Coderre, 1996; Neugebauer et al., 1999; Karim et al., 2001). In the present study, the pretreatment of mGluR1 or mGluR5 antagonists significantly delayed the development of mechanical hyperalgesia and allodynia after inflammation. Similar to the effect of the NMDAR antagonist (Ren et al., 1992), the group I mGluR antagonists did not produce an effect on the noninflamed paw, suggesting a selective effect on hyperalgesia. Intrathecal administration of the IP_3 receptor antagonist also produced a similar effect. Importantly, the same dose of these mGluR antagonists selectively blocked inflammation-induced, but not basal levels of, NR2B tyr-P. Our results also suggest that the postsynaptic mGluR-NMDAR coupling after inflammation mainly occurs in the initiation phase of dorsal horn hyperexcitability, because the post-treatment of the mGluR antagonists only produced a minor effect. Other signaling pathways may be more important for the maintenance of persistent sensitization. It was noted in the present study that antagonists of mGluR1 and mGluR5 each individually blocked NR2B tyr-P and attenuated behavioral hyperalgesia. Although these results suggest that the involvement of both group I mGluR subtypes is necessary in coupling NMDAR signaling, the molecular mechanisms underlying this phenomenon is unclear. One attractive speculation related to these results is the oligomerization of the mGluRs. G-protein-coupled receptors form oligomeric assemblies, and many of them exist as homodimers and heterodimers (Terrillon and Bouvier, 2004). Increasing evidence indicates that oligomerization of G-protein-coupled receptors plays an important role in receptor function. The homodimers of mGluR1 and mGluR5 have been demonstrated previously (Romano et al., 1996; Kunishima et al., 2000). However, heteromeric mGluRs have not been reported. This phenomenon deserves additional study.

The present study indicates that the IP_3-mediated intracellular calcium release is necessary and sufficient for downstream NR2B tyr-P associated with hyperalgesia. The application of IP_3 receptor antagonists blocked NR2B tyr-P induced by inflammation *in vivo* and group I mGluR agonists *in vitro*, suggesting a critical role of the intracellular calcium release. In contrast, blockage of other potential calcium sources, including NMDA and AMPA/KA receptor channels, and VDCCs was without an effect on NR2B tyr-P. It is rather surprising that in the present study, MK-801, an NMDAR channel blocker, did not prevent NR2B

tyr-P after inflammation, although the doses used have been shown to attenuate hyperalgesia (Ren et al., 1992). This suggests that the NMDAR channel itself does not contribute to the initiation of the increased NR2B tyr-P through a feedforward mechanism. In hippocampus, the increased NR2B tyr-P was observed after the establishment of long-term potentiation and blocked by MK-801 (Rosenblum et al., 1996; Rostas et al., 1996), suggesting that tyr-P after tetanus is triggered by activation of the NMDAR itself. These apparent contrasting results emphasize the differences in biochemical signaling among different cellular systems. Our MK-801 result suggests that tyr-P of the NMDAR does not depend on the opening status of the NMDAR channel, and MK-801 produces antihyperalgesic effects by acting on an event downstream to initiation of NR2B tyr-P.

The unique contribution of IP_3 receptor-mediated calcium release to NR2B tyr-P raises interesting questions on intracellular calcium signaling and spinal dorsal horn plasticity. Despite multiple calcium sources, our results suggest that the signal pathways upstream to NR2B tyr-P depend on calcium released from the endoplasmic reticulum. Compared with synaptic response involving ionotropic glutamate receptors, the calcium release from the endoplasmic reticulum following mGluR activation exhibits a considerable delay of ~200 msec in Purkinje cells in the mouse cerebellum (Takechi et al., 1998). Nakamura et al. (1999) have shown a difference between the spatial distributions of the NMDAR-mediated calcium changes and mGluR-mediated release, suggesting that these two spatially distinct calcium changes may serve different functions. Compared with calcium release resulting from action potentials, the IP_3-mediated intracellular calcium release after mGluR activation is much larger and requires repetitive synaptic stimulation (Nakamura et al., 1999). Because hindpaw inflammation produces a strong primary afferent barrage to dorsal horn neurons followed by mGluR activation, it may satisfy the condition for subsequent "spatially limited" or "functionally compartmentalized" intracellular calcium release that leads to NR2B tyr-P.

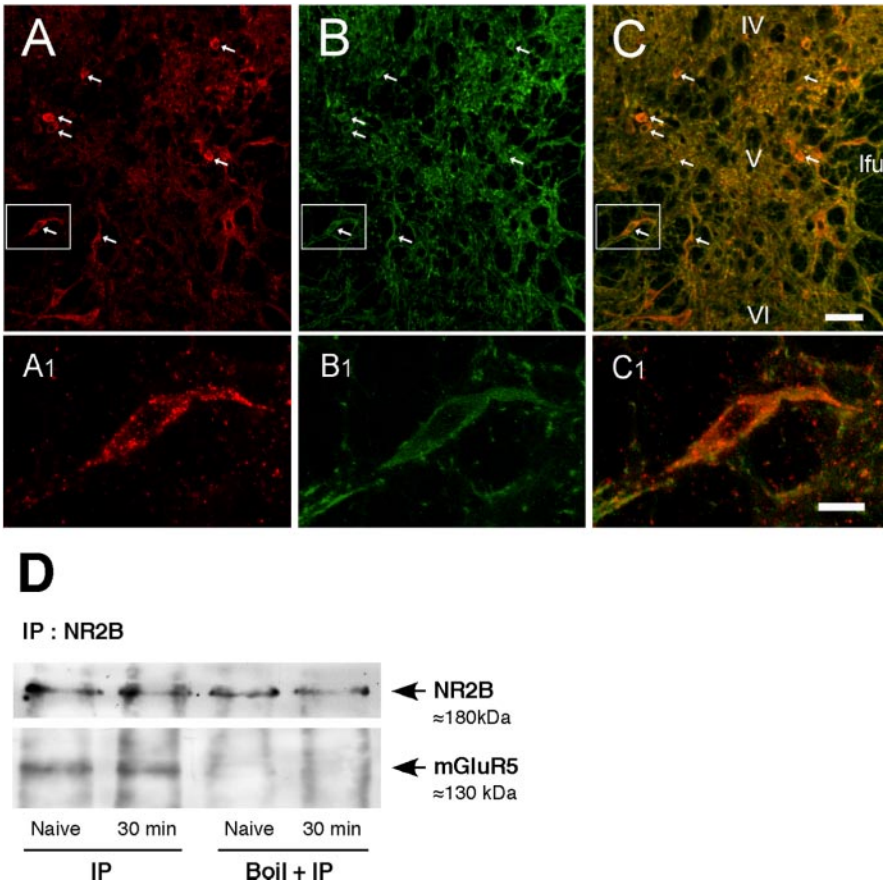

Figure 8. Colocalization of NMDAR and mGluR5 in the spinal dorsal horn. *A*, NMDAR NR1 subunit-like immunoreactivity is visualized with Cy3-tyramide (red). *B*, mGluR5-like immunoreactivity is shown as green fluorescence after reacting with goat anti-rabbit IgG conjugated to Alexa Fluor 488. *C*, Overlap of panels *A* and *B* illustrating dorsal horn neurons that exhibit double fluorescence (yellow-orange; arrows), suggesting colocalization of NMDAR/mGluR5. The area shown includes laminas IV-VI of the lateral spinal dorsal horn medial to the lateral funiculus (lfu). A_1, B_1, and C_1 are enlarged from rectangles in *A*, *B*, and *C*, respectively. The NR1 staining showed numerous punctate profiles in the cell membrane, dendrite, and cytoplasm (A_1), whereas mGluR5-like immunoreactivity appeared uniformly in the cell membrane and cytoplasm (B_1). C_1 shows the same neuron in A_1 and B_1 that is double labeled with anti-NR1 and mGluR5 antibodies. Scale bars: *A–C*, 0.04 mm; A_1–C_1, 0.01 mm. *D*, Coimmunoprecipitation of NR2B and mGluR5 in the spinal dorsal horn. Spinal dorsal horn tissues were taken from naive rats and inflamed rats at 30 min after injection of CFA into the hindpaw. Proteins were immunoprecipitated with NR2B antibodies and probed with antibodies against NR2B and mGluR5. Note that boiling of the samples before IP eliminated mGluR5, leaving only NR2B that was directly pulled down by NR2B antibodies.

Although the communication between mGluR and NMDARs and tyr-P of the NMDAR in the postsynaptic density may be a general mechanism for synaptic modulation, different cellular systems may involve different receptor subunit and distinct second messenger pathways. For example, NR2A tyr-P is upregulated in the rostral ventromedial medulla, a pivotal structure for pain modulation, after inflammation (Turnbach et al., 2003), whereas the level of NR2A tyr-P was unchanged at the spinal level (Guo et al., 2002a). Our analysis indicates that both mGluR1 and mGluR5 subtypes of group I mGluRs were required for enhanced NR2B tyr-P and PKC activation, and intracellular calcium release is critical for this effect. In cortical neurons, however, tyr-P of the NMDAR NR2A/B subunits following activation of group I mGluRs was blocked by an mGluR1, but not mGluR5, antagonist, and the activation of PYK2/Src kinase by mGluR agonist DHPG did not appear to depend on PKC but was dependent on Ca^{2+}-calmodulin (Heidinger et al., 2002). In addition, the activation of spinal neurokinin 1 receptors also appears to be involved in CFA-induced NR2B tyr-P (Guo et al., 2002a), suggesting the presence of abundant signaling pathways in the spinal cord.

In summary, these findings demonstrate an mGluR-NMDAR coupling in the spinal dorsal horn involving IP_3-mediated intracellular calcium release, PKC activation, and Src-induced NR2B tyr-P. These biochemical events are correlated with the development of inflammatory hyperalgesia and may underlie the mechanisms of spinal sensitization. An important implication from the present study is that mGluR facilitates ionotropic synaptic transmission after injury as a mechanism of modulation in the spinal dorsal horn. It is known that tyr-P of the NMDAR results in an increase in NMDAR channel current and Ca^{2+} influx

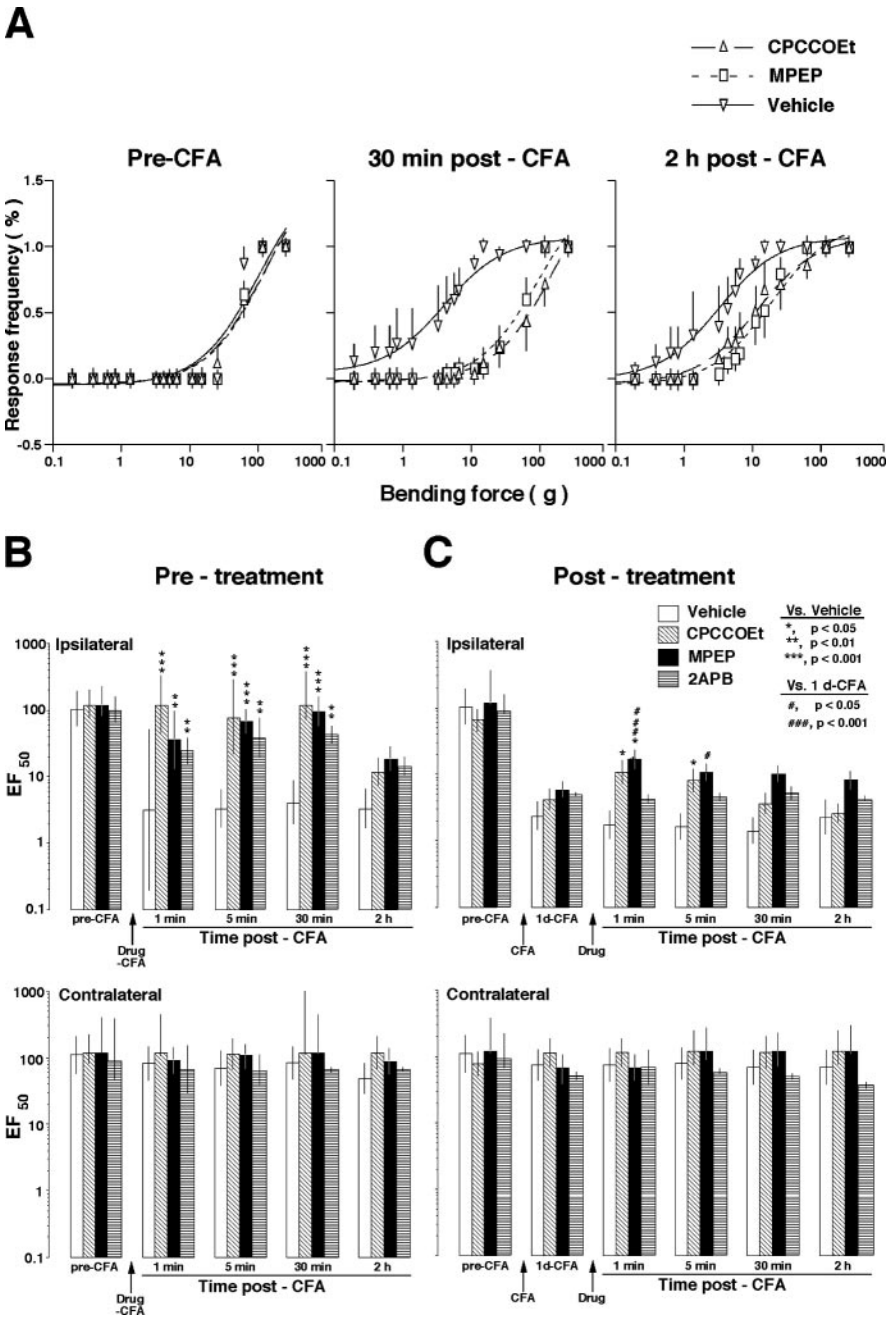

Figure 9. Effects of selective group I mGluR antagonists on inflammatory hyperalgesia–allodynia. *A*, Stimulus–response frequency curves illustrating examples of the intensity-dependent paw withdrawal responses to mechanical stimuli. Each curve was established with a series of subthreshold to suprathreshold range of von Frey filament forces, and the response frequency is plotted against the stimulus intensity. Inflammation was induced in the left hindpaw. The stimulus–response curves for vehicle, CPCCOEt (mGluR1 antagonist), and MPEP (mGluR5 antagonist) overlapped before inflammation (pre-CFA), indicating consistent responses. There was a leftward shift of the curve in vehicle-treated rats at 30 min post-CFA, compared with the pre-CFA curve, suggesting the development of mechanical hyperalgesia and allodynia. At 30 min post-CFA in CPCCOEt- and MPEP-treated rats, the stimulus–response curves were shifted to the right compared with vehicle-treated rats, suggesting an attenuation of hyperalgesia–allodynia. At 2 hr post-CFA, the curves shifted back to the left in CPCCOEt- and MPEP-treated rats as hyperalgesia was recovering from the drug effect. *B*, EF_{50} values, defined as the von Frey filament force (*g*) that produces a 50% response frequency, were derived from the stimulus–response function curve and used as a measure of mechanical sensitivity. Pretreatment (10 min before CFA) of rats with CPCCOEt (2 μmol; $n = 5$), MPEP (170 nmol; $n = 5$), or 2APB (1 nmol; $n = 6$) prevented the early development of hyperalgesia–allodynia on the inflamed paw as shown by significantly higher EF_{50} values when compared with vehicle-treated rats (DMSO; 0.01 ml; $n = 4$). The responses of the contralateral noninflamed paw were not affected by the drug treatment. *C*, CPCCOEt (2 μmol; $n = 4$), MPEP (170 nmol; $n = 5$), or 2APB (1 nmol; $n = 6$) were administered intrathecally at 1 d post-CFA when mechanical hyperalgesia–allodynia had developed. There was a slight increase in EF_{50} values that lasted for ~5 min after CPCCOEt and MPEP treatment. The 95% confidence limit of the EF_{50} values is shown as a vertical line in each bar in *B* and *C*.

through the channel (Wang and Salter, 1994; Ali and Salter, 2001). Thus, one functional consequence of mGluR activation after inflammation is to prime NMDAR for further enhanced hyperexcitability. This mechanism may be a critical initiator for central nociceptive sensitization.

References

Ali DW, Salter MW (2001) NMDA receptor regulation by Src kinase signaling in excitatory synaptic transmission and plasticity. Curr Opin Neurobiol 11:336–342.

Benquet P, Gee CE, Gerber U (2002) Two distinct signaling pathways upregulate NMDA receptor responses via two distinct metabotropic glutamate receptor subtypes. J Neurosci 22:9679–9686.

Bleakman D, Rusin KI, Chard PS, Glaum SR, Miller RJ (1992) Metabotropic glutamate receptors potentiate ionotropic glutamate responses in the rat dorsal horn. Mol Pharmacol 42:192–196.

Bond A, Lodge D (1995) Pharmacology of metabotropic glutamate receptor-mediated enhancement of responses to excitatory and inhibitory amino acids on rat spinal neurones *in vivo*. Neuropharmacology 34:1015–1023.

Boxall SJ, Berthele A, Tolle TR, Zieglgansberger W, Urban L (1998) mGluR activation reveals a tonic NMDA component in inflammatory hyperalgesia. NeuroReport 9:1201–1203.

Boyce S, Wyatt A, Webb JK, O'Donnell R, Mason G, Rigby M, Sirinathsinghji D, Hill RG, Rupniak NM (1999) Selective NMDA NR2B antagonists induce antinociception without motor dysfunction: correlation with restricted localisation of NR2B subunit in dorsal horn. Neuropharmacology 38:611–623.

Burette A, Wyszynski M, Valtschanoff JG, Sheng M, Weinberg RJ (1999) Characterization of glutamate receptor interacting protein-immunopositive neurons in cerebellum and cerebral cortex of the albino rat. J Comp Neurol 411:601–612.

Cerne R, Randic M (1992) Modulation of AMPA and NMDA responses in rat spinal dorsal horn neurons by trans-1-aminocyclopentane-1,3-dicarboxylic acid. Neurosci Lett 144:180–184.

Dikic I, Tokiwa G, Lev S, Courtneidge SA, Schlessinger J (1996) A role for Pyk2 and Src in linking G-protein-coupled receptors with MAP kinase activation. Nature 383:547–550.

Dolan S, Nolan AM (2002) Behavioral evidence supporting a differential role for spinal group I and II metabotropic glutamate receptors in inflammatory hyperalgesia in sheep. Neuropharmacology 43:319–326.

Dubner R, Ruda MA (1992) Activity-dependent neuronal plasticity following tissue injury and inflammation. Trends Neurosci 15:96–103.

Engelman HS, Allen TB, MacDermott AB (1999) The distribution of neurons expressing calcium-permeable AMPA receptors in the superficial laminae of the spinal cord dorsal horn. J Neurosci 19:2081–2089.

Fisher K, Coderre TJ (1996) The contribution of metabotropic glutamate receptors (mGluRs) to formalin-induced nociception. Pain 68:255–263.

Guo W, Zou S, Guan Y, Ikeda T, Tal M, Dubner R, Ren K (2002a) Tyrosine phosphorylation of the NR2B subunit of the NMDA receptor in the spinal cord during the development and maintenance of inflammatory hyperalgesia. J Neurosci 22:6208–6217.

Guo W, Zou S, Tal M, Ren K (2002b) Activation of spinal kainate receptors after inflammation: behavioral hyperalgesia and subunit gene expression. Eur J Pharmacol 45:309–318.

Haley JE, Sullivan AF, Dickenson AH (1990) Evidence of spinal *N*-methyl-D-aspartate receptor involvement in prolonged chemical nociception in the rat. Brain Res 518:218–226.

Heidinger V, Manzerra P, Wang XQ, Strasser U, Yu SP, Choi DW, Behrens MM (2002) Metabotropic glutamate receptor 1-induced upregulation of NMDA receptor current: mediation through the Pyk2/Src-family kinase pathway in cortical neurons. J Neurosci 22:5452–5461.

Huang Y, Lu W, Ali DW, Pelkey KA, Pitcher GM, Lu YM, Aoto H, Roder JC, Sasaki T, Salter MW, MacDonald JF (2001) CAKbeta/Pyk2 kinase is a signaling link for induction of long-term potentiation in CA1 hippocampus. Neuron 29:485–496.

Hudson LJ, Bevan S, McNair K, Gentry C, Fox A, Kuhn R, Winter J (2002) Metabotropic glutamate receptor 5 upregulation in A-fibers after spinal nerve injury: 2-methyl-6-(phenylethynyl)-pyridine (MPEP) reverses the induced thermal hyperalgesia. J Neurosci 22:2660–2668.

Hunt SP, Mantyh PW (2001) The molecular dynamics of pain control. Nat Rev Neurosci 2:83–91.

Husi H, Ward MA, Choudhary JS, Blackstock WP, Grant SG (2000) Proteomic analysis of NMDA receptor-adhesion protein signaling complexes. Nat Neurosci 37:661–669.

Hylden JLK, Nahin RL, Traub RJ, Dubner R (1989) Expansion of receptive fields of spinal lamina I projection neurons in rats with unilateral adjuvant-induced inflammation: the contribution of dorsal horn mechanisms. Pain 37:229–243.

Iadarola MJ, Brady LS, Draisci G, Dubner R (1988) Enhancement of dynorphin gene expression in spinal cord following experimental inflammation: stimulus specificity, behavioral parameters and opioid receptor binding. Pain 35:313–326.

Ji RR, Woolf CJ (2001) Neuronal plasticity and signal transduction in nociceptive neurons: implications for the initiation and maintenance of pathological pain. Neurobiol Dis 8:1–10.

Ji RR, Baba H, Brenner GJ, Woolf CJ (1999) Nociceptive-specific activation of ERK in spinal neurons contributes to pain hypersensitivity. Nat Neurosci 2:1114–1119.

Karim F, Wang CC, Gereau IV RW (2001) Metabotropic glutamate receptor subtypes 1 and 5 are activators of extracellular signal-regulated kinase signaling required for inflammatory pain in mice. J Neurosci 21:3771–3779.

Kunishima N, Shimada Y, Tsuji Y, Sato T, Yamamoto M, Kumasaka T, Nakanishi S, Jingami H, Morikawa K (2000) Structural basis of glutamate recognition by a dimeric metabotropic glutamate receptor. Nature 407:971–977.

Lan JY, Skeberdis VA, Jover T, Zheng X, Bennett MV, Zukin RS (2001) Activation of metabotropic glutamate receptor 1 accelerates NMDA receptor trafficking. J Neurosci 21:6058–6068.

Lei G, Xue S, Chery N, Liu Q, Xu J, Kwan CL, Fu YP, Lu YM, Liu M, Harder KW, Yu XM (2002) Gain control of *N*-methyl-D-aspartate receptor activity by receptor-like protein tyrosine phosphatase alpha. EMBO J 21:2977–2989.

Lorrain DS, Correa L, Anderson J, Varney M (2002) Activation of spinal group I metabotropic glutamate receptors in rats evokes local glutamate release and spontaneous nociceptive behaviors: effects of 2-methyl-6-(phenylethynyl)-pyridine pretreatment. Neurosci Lett 327:198–202.

Malenka RC, Nicoll RA (1999) Long-term potentiation–a decade of progress? Science 285:1870–1874.

Malmberg AB, Yaksh TL (1994) Voltage-sensitive calcium channels in spinal nociceptive processing: blockade of N- and P-type channels inhibits formalin-induced nociception. J Neurosci 14:4882–4890.

Maruyama T, Kanaji T, Nakade S, Kanno T, Mikoshiba K (1997) 2APB, 2-aminoethoxydiphenyl borate, a membrane-penetrable modulator of Ins(1,4,5)P3-induced Ca^{2+} release. J Biochem (Tokyo) 122:498–505.

Matthews EA, Dickenson AH (2001) Effects of spinally delivered N- and P-type voltage-dependent calcium channel antagonists on dorsal horn neuronal responses in a rat model of neuropathy. Pain 92:235–246.

McCallum JB, Kwok WM, Mynlieff M, Bosnjak ZJ, Hogan QH (2003) Loss of T-type calcium current in sensory neurons of rats with neuropathic pain. Anesthesiology 98:209–216.

Meller ST, Dykstra CL, Gebhart GF (1993) Acute mechanical hyperalgesia is produced by coactivation of AMPA and metabotropic glutamate receptors. NeuroReport 4:879–882.

Mills CD, Xu GY, Johnson KM, McAdoo DJ, Hulsebosch CE (2000) AIDA reduces glutamate release and attenuates mechanical allodynia after spinal cord injury. NeuroReport 11:3067–3070.

Morisset V, Nagy F (1996) Modulation of regenerative membrane properties by stimulation of metabotropic glutamate receptors in rat deep dorsal horn neurons. J Neurophysiol 76:2794–2798.

Naisbitt S, Kim E, Tu JC, Xiao B, Sala C, Valtschanoff J, Weinberg RJ, Worley PF, Sheng M (1999) Shank, a novel family of postsynaptic density proteins that binds to the NMDA receptor/PSD-95/GKAP complex and cortactin. Neuron 23:569–582.

Nakamura T, Barbara JG, Nakamura K, Ross WN (1999) Synergistic release of Ca^{2+} from IP_3-sensitive stores evoked by synaptic activation of mGluRs paired with backpropagating action potentials. Neuron 24:727–737.

Neugebauer V (2002) Metabotropic glutamate receptors–important modulators of nociception and pain behavior. Pain 98:1–8.

Neugebauer V, Chen PS, Willis WD (1999) Role of metabotropic glutamate receptor subtype mGluR1 in brief nociception and central sensitization of primate STT cells. J Neurophysiol 82:272–282.

O'Connor JJ, Rowan MJ, Anwyl R (1994) Long-lasting enhancement of NMDA receptor-mediated synaptic transmission by metabotropic glutamate receptor activation. Nature 367:557–579.

Ren K (1999) An improved method for assessing mechanical allodynia in the rat. Physiol Behav 67:711–716.

Ren K, Dubner R (1999) Central nervous system plasticity and persistent pain. J Orofacial Pain 13:155–163.

Ren K, Hylden JLK, Williams GM, Ruda MA, Dubner R (1992) The effects of a non-competitive NMDA receptor antagonist, MK-801, on behavioral hyperalgesia and dorsal horn neuronal activity in rats with unilateral inflammation. Pain 50:331–344.

Romano C, Yang WL, O'Malley KL (1996) Metabotropic glutamate receptor 5 is a disulfide-linked dimer. J Biol Chem 271:28612–28616.

Rosenblum K, Dudai Y, Richter-Levin G (1996) Long-term potentiation increases tyrosine phosphorylation of the *N*-methyl-D-aspartate receptor subunit 2B in rat dentate gyrus *in vivo*. Proc Natl Acad Sci USA 93:10457–10460.

Rostas JA, Brent VA, Voss K, Errington ML, Bliss TV, Gurd JW (1996) Enhanced tyrosine phosphorylation of the 2B subunit of the *N*-methyl-D-aspartate receptor in long-term potentiation. Proc Natl Acad Sci USA 93:10452–10456.

Salter MW (1998) Src, *N*-methyl-D-aspartate (NMDA) receptors, and synaptic plasticity. Biochem Pharmacol 56:789–798.

Shindler KS, Roth KA (1996) Double immunofluorescent staining using two unconjugated primary antisera raised in the same species. J Histochem Cytochem 44:1331–1335.

Skeberdis VA, Lan J, Opitz T, Zheng X, Bennett MV, Zukin RS (2001) mGluR1-mediated potentiation of NMDA receptors involves a rise in intracellular calcium and activation of protein kinase C. Neuropharmacology 40:856–865.

Solovyova N, Verkhratsky A (2003) Neuronal endoplasmic reticulum acts as a single functional Ca^{2+} store shared by ryanodine and inositol-1,4,5-trisphosphate receptors as revealed by intra-ER $[Ca^{2+}]$ recordings in single rat sensory neurones. Pflügers Arch 446:447–454.

Takechi H, Eilers J, Konnerth A (1998) A new class of synaptic response involving calcium release in dendritic spines. Nature 396:757–760.

Tao YX, Huang YZ, Mei L, Johns RA (2000) Expression of PSD-95/SAP90 is critical for *N*-methyl-D-aspartate receptor-mediated thermal hyperalgesia in the spinal cord. Neuroscience 98:201–206.

Terrillon S, Bouvier M (2004) Roles of G-protein-coupled receptor dimerization. EMBO J 5:30–34.

Tezuka T, Umemori H, Akiyama T, Nakanishi S, Yamamoto T (1999) PSD-95 promotes Fyn-mediated tyrosine phosphorylation of the *N*-methyl-D-aspartate receptor subunit NR2A. Proc Natl Acad Sci USA 96:435–440.

Tu JC, Xiao B, Naisbitt S, Yuan JP, Petralia RS, Brakeman P, Doan A, Aakalu VK, Lanahan AA, Sheng M, Worley PF (1999) Coupling of mGluR/

Homer and PSD-95 complexes by the Shank family of postsynaptic density proteins. Neuron 23:583–592.

Turnbach ME, Guo W, Dubner R, Ren K (2003) Inflammation induces tyrosine phosphorylation of the NR2A subunit and serine phosphorylation of NR1 subunits in the rat rostral ventromedial medulla. Soc Neurosci Abstr 29:695.13.

Walker K, Bowes M, Panesar M, Davis A, Gentry C, Kesingland A, Gasparini F, Spooren W, Stoehr N, Pagano A, Flor PJ, Vranesic I, Lingenhoehl K, Johnson EC, Varney M, Urban L, Kuhn R (2001) Metabotropic glutamate receptor subtype 5 (mGlu5) and nociceptive function. I. Selective blockade of mGlu5 receptors in models of acute, persistent and chronic pain. Neuropharmacology 40:1–9.

Wang YT, Salter MW (1994) Regulation of NMDA receptors by tyrosine kinases and phosphatases. Nature 369:233–235.

Woolf CJ, Salter MW (2000) Neuronal plasticity: increasing the gain in pain. Science 288:1765–1768.

Woolf CJ, Thompson SWN (1991) The induction and maintenance of central sensitization is dependent on *N*-methyl-D-aspartic acid receptor activation; implications for the treatment of post-injury pain hypersensitivity states. Pain 44:293–299.

Yaksh TL, Rudy TA (1976) Chronic catheterization of the spinal subarachnoid space. Physiol Behav 17:1031–1036.

Yu XM, Askalan R, Keil Jr GJ, Salter MW (1997) NMDA channel regulation by channel-associated protein tyrosine kinase Src. Science 275:674–678.

Zhang L, Lu Y, Chen Y, Westlund KN (2002) Group I metabotropic glutamate receptor antagonists block secondary thermal hyperalgesia in rats with knee joint inflammation. J Pharmacol Exp Ther 300:149–156.